

Supplemental Material and Methods

Quantification of calbindin intensity

The intensity of immunohistological staining for calbindin was determined in the area of intrafusal fibers using ImageJ software 1.46j, and expressed as integrated density per intrafusal fiber. Data were gathered from sections using 15-20 muscle spindles/animal, 4 to 8 animals per genotype. Data are plotted as mean \pm SEM.

Analysis of g-ratio

The inner (axon) and outer (axon+myelin) perimeter of 125 to 275 myelinated axons were determined from electron microscopy pictures of sciatic nerves from P12 (co-IgNrg1 strain) or P180 (coErbB2 and Bace1^{-/-} strains) animals, expressed as mean \pm SEM (coErbB2, Bace1^{-/-}) or plotted against axon diameter (Fig. S5C).

Supplemental Figure legends

Figure S1 Quantification of motor coordination defects

(A-C) The deviation from the ideal homolateral (A) and homolog (B,C) coordination value (0.5) was plotted for the different mutants. **(A)** Ly2811376-treated, co-IgNrg1 and Bace1^{-/-} mice show significantly increased deficits in homolateral coordination compared to control animals. **(B,C)** Only co-IgNrg1 mice show significantly altered homolog coordination that is more pronounced on hindlimb than forelimb level.

Figure S2 Inhibition of Bace1 in the adult mouse

(A) Performance of Bace1^{-/-} and coErbB2 (Krox20^{cre/+}ErbB2^{flox/flox}) mutants compared to their respective littermates in the inverted grid test. coErbB2 and Bace1^{-/-} mice display hypomyelination of peripheral nerves (g-ratios, P180: control, Bace1^{-/-} and coErbB2: 0.68±0.01, 0.75±0.01 and 0.80±0.01, respectively). However, in contrast to Bace1^{-/-} mutants the grip ability of coErbB2 mice is unaffected. **(B)** Representative walking patterns of coErbB2 mutants and their littermates. **(C,D)** Homolateral (C) and homolog (D) coupling values for the movements of control (inner circle) and coErbB2 (outer circle) mice. Bace1^{-/-} mice (middle circle) are included for comparison. **(E)** 3D reconstruction of the tibialis anterior muscle from Bace1^{+/+}, Bace1^{+/-} and Bace1^{-/-} animals treated with the Bace1 inhibitor Ly2811376. White lines indicate the muscle spindles. Scale Bar: 1.5 mm (E).

Figure S3 Nrg1 isotypes and schematic display of mutant alleles

(A) Schematic representation of Nrg1 isotypes. The amino-terminal part of the EGF domain of Nrg1 proteins is constant, while their carboxy-terminal sequence varies due to alternative splicing of the corresponding transcripts. Six distinct isotypes (from top to bottom, α1/2, β1-4) were described in mice. **(B)** Schematic display of IgNrg1^{flox} and Nrg1^{flox} alleles before and after cre-mediated recombination. **IgNrg1^{flox}**: LoxP sequences (green arrowheads) were inserted upstream and downstream of the exon encoding the Ig2 domain (exon 4; ENSEMBL database). Cre-mediated recombination removes exon 4, introducing a frameshift in all IgNrg1 mRNAs. **Nrg1^{flox}**: LoxP

sequences were inserted upstream and downstream of exons encoding the α , β and isotype 3 of the EGF domain of Nrg1 (exon 9-11, ENSEMBL database). Cre-mediated recombination prevents transcription of sequences encoding a complete EGF domain, and introduces frameshifts that result in the early termination of all Nrg1 mRNAs.

Figure S4 Nrg1 isoforms and muscle spindles in IgNrg1 mutants

(A) Quantification (qPCR) of the transcripts encoding CRD and IgNrg1 isoforms in DRG neurons from control, IgNrg1 $\Delta^{+/+}$, co-IgNrg1 and IgNrg1 $\beta 1^{Ov}$ mutants at P0. **(B)** Aberrant curled tail posture (top) and immunohistological analyses of the bicipital tail muscle (bottom) from co-IgNrg1 animals and their littermates. Immunohistology was performed using antibodies directed against Egr3, NF200 and collagen IV to detect the muscle spindle. Note the scarcity of (Egr3 $^{+}$) muscle spindles (arrowheads) in co-IgNrg1 animals compared to their littermates. Scale bar: 50 μ m (B).

Figure S5 Muscle spindle morphology at birth and effect of co-IgNrg1 on myelination

(A) Immunohistological analysis of muscle spindles in newborn mice of indicated genotypes (Bace1 $^{-/-}$ is abbreviated as B1 $^{-/-}$). Intrafusal fibers express Egr3. The nascent capsule displays a pronounced collagen IV staining, and contacting sensory fibers are NF200 $^{+}$. **(B,C)** Electron microscopy pictures of transversal sections (B) and g-ratio distribution (C) of sciatic nerves obtained from control and co-IgNrg1 mice at P12. Orange symbols indicate axons of matching diameters. Scale bar: 10 μ m (A).

Figure S6 Calbindin and S100 expression in intrafusal fibers depends on IgNrg1 dosage

(A) Quantification of the intensity of calbindin staining in intrafusal fibers in mice with the indicated genotypes. **(B)** Immunohistological staining of adult (P30) muscle spindles from hindlimbs of mice with the indicated genotypes. NF200-positive sensory afferents are present in all genotypes. Capsule, terminal Schwann cells and intrafusal fibers express S100. Note that, similar to calbindin, the intensity of S100 staining in intrafusal fibers depends on the IgNrg1 dose. Scale bar: 20 μ m (B).

Figure S7 Video of coTxNrg1 and control mice walking on a beam

The video was slowed down from 25 fps to 10 fps to ease visualization. Left and Right steps are indicated in the top part of the video, following this notation: correct step (+), missed step (X), hopping movement (h).

Supplemental table I Primer pairs used for qPCR experiments

The sequences of primers used for quantification of Nrg1 isoforms and subtypes analysis are listed. The primers recognize sequences encoding particular domains (EGF variants, CRD, Ig2, TM), as indicated (cf. Falls, 2003). Some primers recognize sequences located on 2 exons; in these primers, sequences corresponding to the 5' exon are shown in italics.

Supplemental table II Statistical analysis of muscle spindle numbers

Analyzed were the results of the quantification shown in Fig. 5A on hindlimbs of newborn mice. The significance of differences was determined using unpaired Student's t-test.

Fig. S1

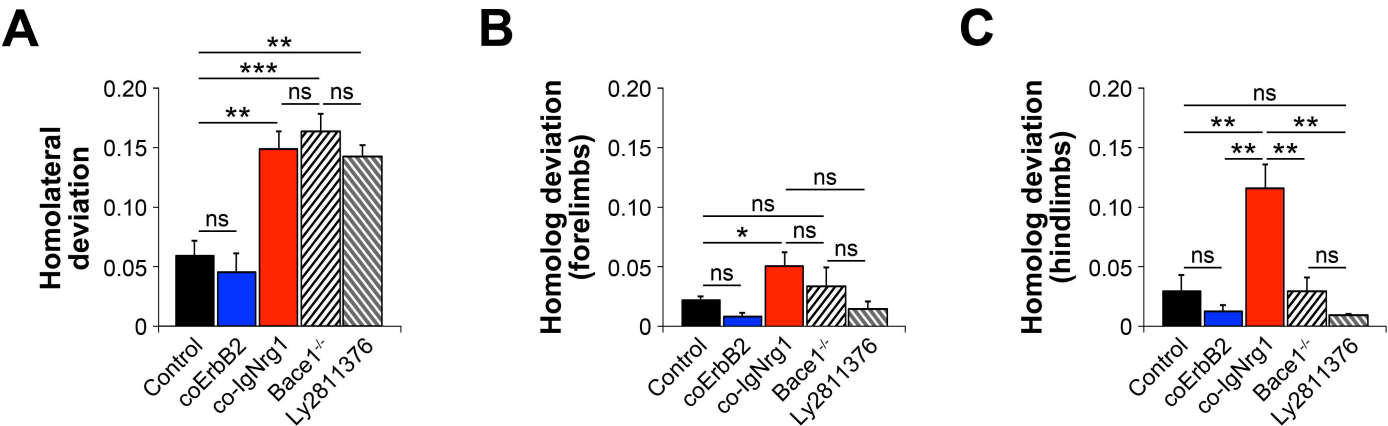


Fig. S2

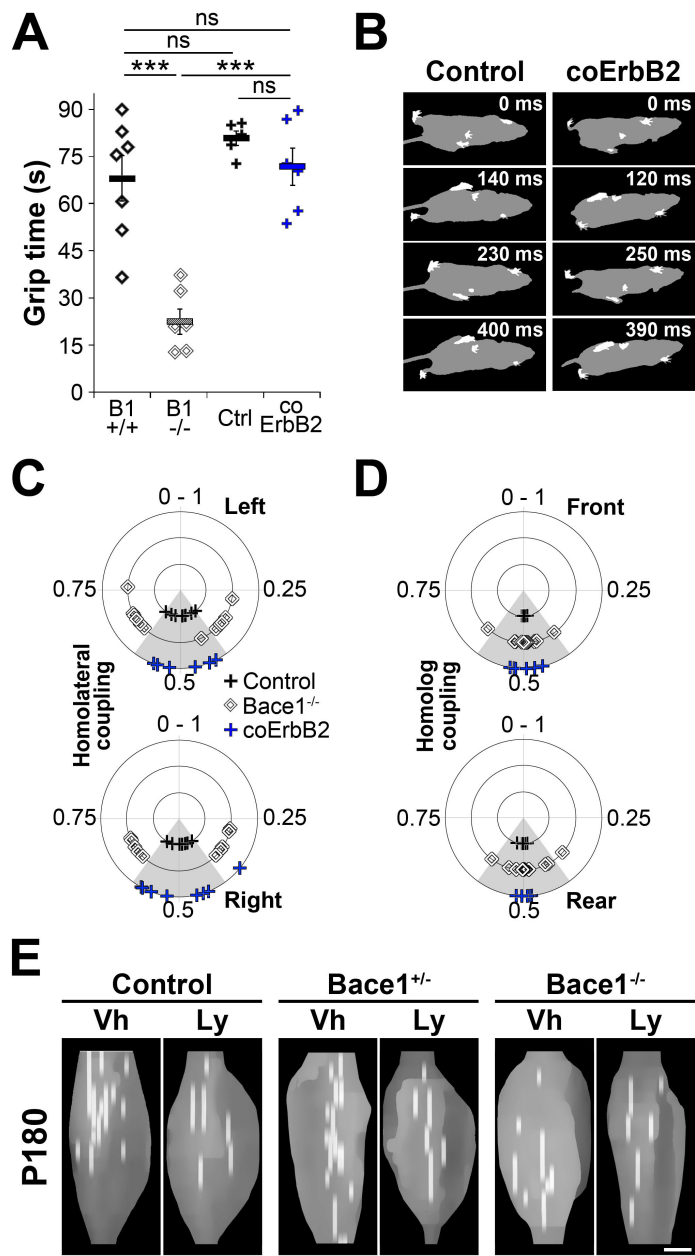


Fig. S3

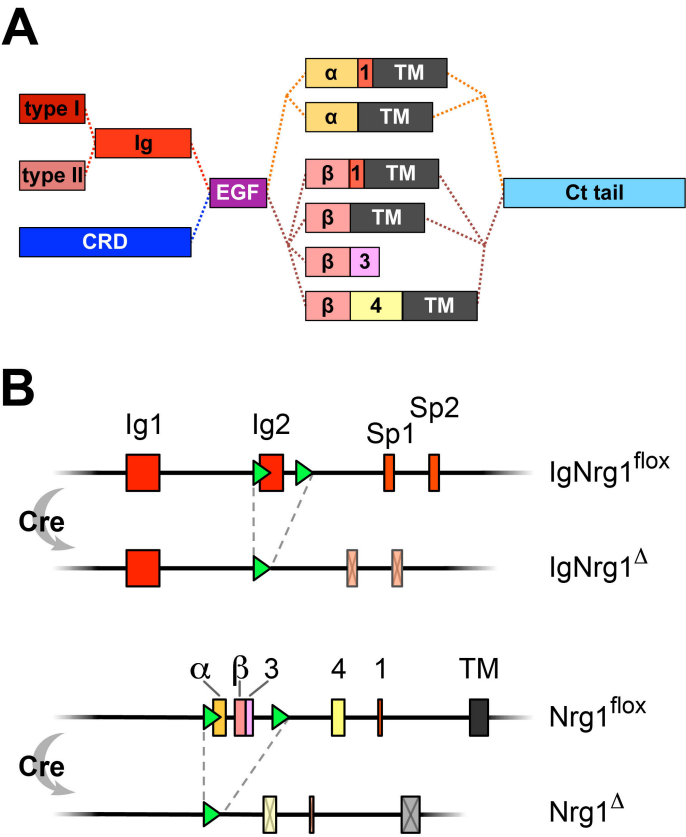


Fig. S4

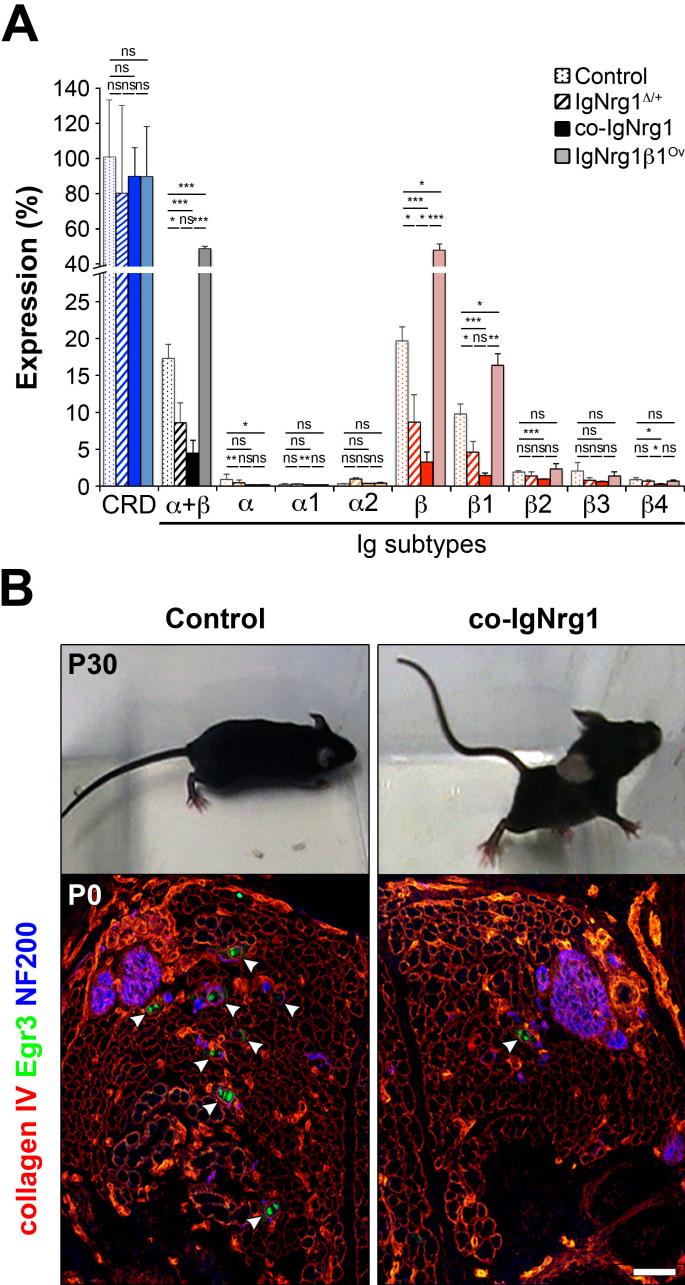


Fig. S5

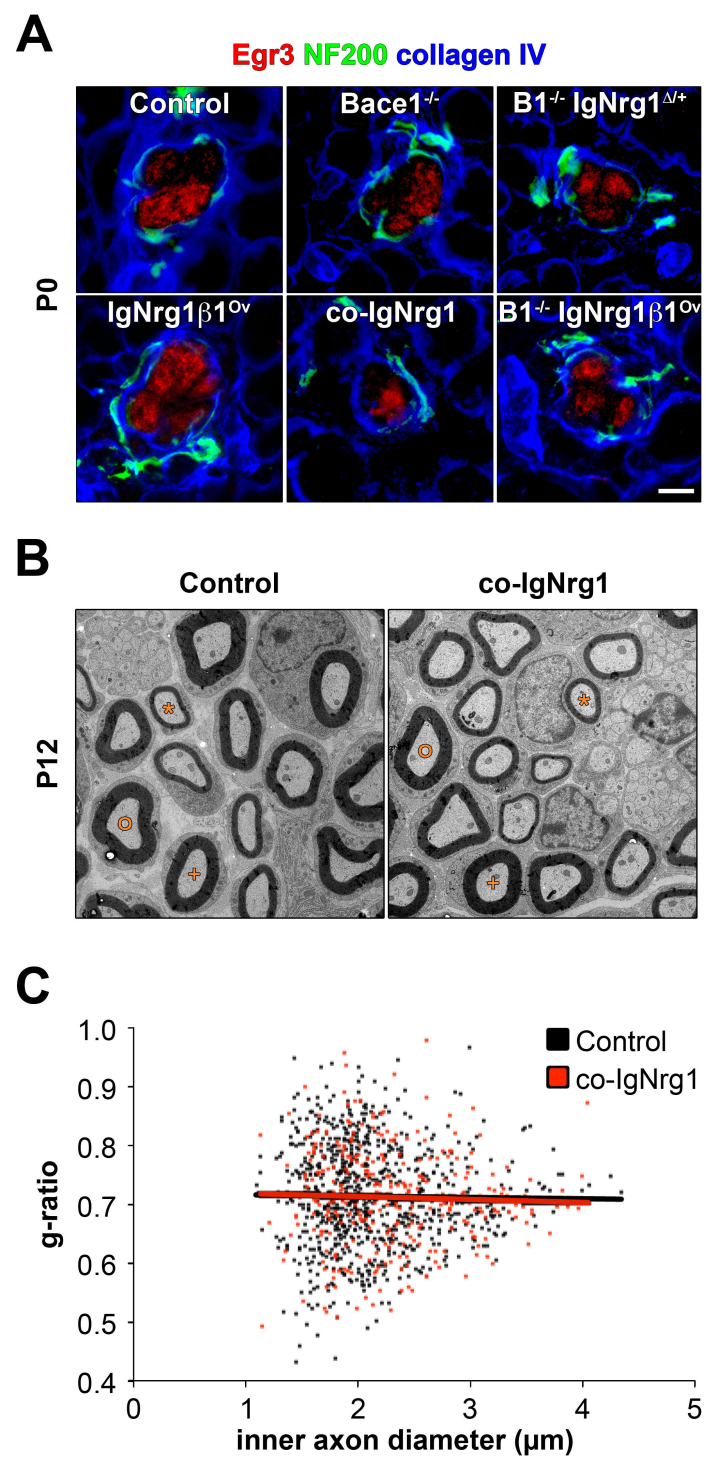
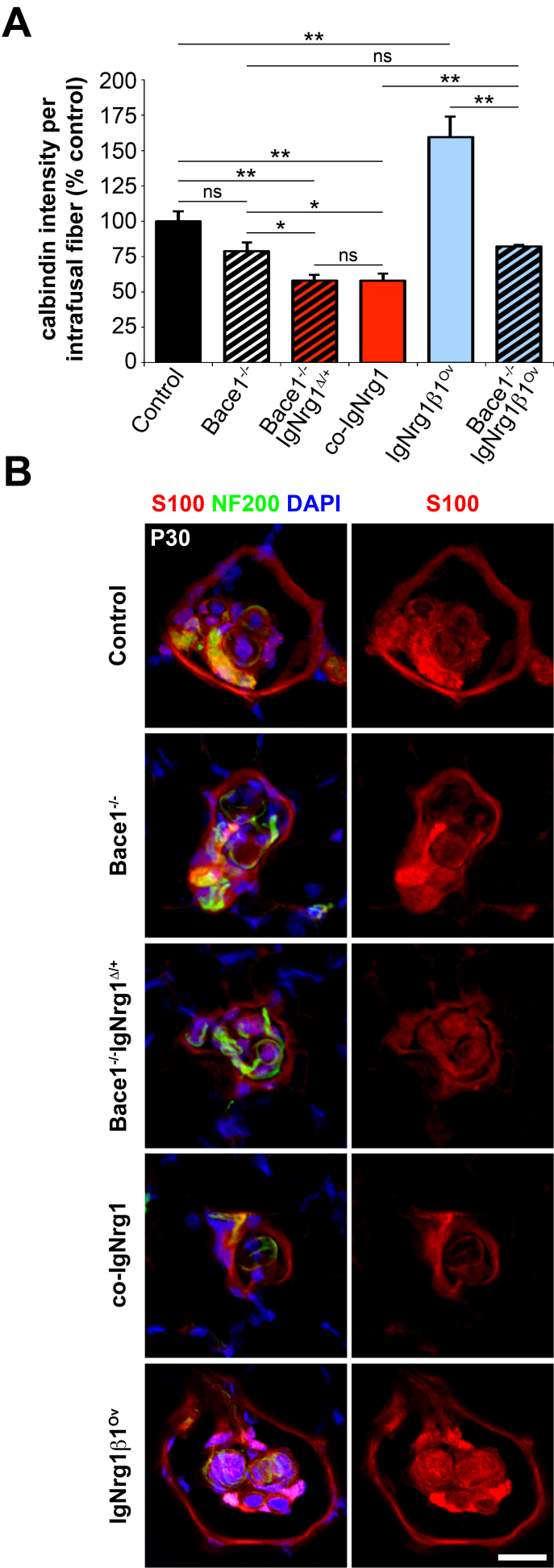


Fig. S6



Supplemental table 1 Primer pairs used for qPCR experiments

Target	Forward primer		Reverse primer		Annealing T°
	Exon	Sequence	Exon	Sequence	
Nrg1-beta	EGF beta	CGTAATGGCCAGCTTCTACA	TM domain	CCATGTTGTTTCGTTCTGACC	60°C
CRD-Nrg1	CRD	CGCTGTTCTGGTCTCATCCG	TM domain	TGCCAGTAATTGTCAGTACCCCTC	55°C
Ig- alpha+beta	Ig2	TGACTCTGGAGAAATATATGTGCAA	TM domain	GCCAGTAATTGTCAGTACCCCTC	55°C
	Ig2	GAATCAACAAAGCGTCCCT	EGF alpha	CATCTTGCTCCAGTGAATCCAG	55°C
Ig- alpha1	Ig2	ACTCTGGAGAAATATATGTGCAA	EGF alpha - <i>EGF 1</i> AAGATGCT TTTCTTGGGTTTG		55°C
alpha2	Ig2	TATATGTGCAAAAGTGATCAGC	EGF alpha - <i>EGF 2</i> CTCCGCTT TTTCTTGGGTT		55°C
beta	Ig2	CTTCGAATCAACAAAGCGTCCC	EGF beta	CGTAGTTTTGGCAACGATCACC	55°C
beta1	Ig2	AGTCAGAGCTTCGAATCAACA	EGF beta - <i>EGF 1</i> CCAAGATGCT TGAGAAAGCTG		55°C
Ig- beta2	Ig2	CTTCGAATCAACAAAGCGTCC	EGF beta - <i>EGF 2</i> CCTCCGCTT TGAGAAAGCTG		55°C
beta3	Ig2	AGTCAGAGCTTCGAATCAACA	EGF beta - <i>EGF 3</i> AGTGGACGTA TGAGAAAGCTG		55°C
beta4	Ig2	TCGAATCAACAAAGCGTCC	EGF beta - <i>EGF 4</i> CCTCCTAGAAG TGAGAAAGCTG		55°C
beta-actin		GTCCACACCCGCCACCAGTTC		GGCCTCGTCACCCACATAG	55°C
GAPDH		TGTGTCCGTCGTGGATCTGA		TTGCTGTTGAAGTCGCAGGAG	60°C

Supplemental table II Statistical analysis of muscle spindle numbers

	Control	IgNrg1 ^{Δ/+}	Bace1 ^{-/-}	Bace1 ^{-/-} IgNrg1 ^{Δ/+}	co-IgNrg1	IgNrg1β1 ^{ov}	Bace1 ^{-/-} IgNrg1β1 ^{ov}
Control		0,002	0,000	0,000	0,000	0,001	0,000
IgNrg1 ^{Δ/+}	**		0,017	0,000	0,000	0,000	0,001
Bace1 ^{-/-}	***	*		0,011	0,000	0,000	0,813
Bace1 ^{-/-} IgNrg1 ^{Δ/+}	***	***	*		0,014	0,000	0,001
co-IgNrg1	***	***	***	*		0,000	0,000
IgNrg1β1 ^{ov}	**	***	***	***	***		0,000
Bace1 ^{-/-} IgNrg1β1 ^{ov}	***	***	ns	***	***	***	